Sustainability in Civil Engineering Journal
Volume: 1, Number 2, June 2026
E-ISSN: 3163-5415
Website: https://journalcendekia.com/SICEJ/

Technical feasibility analysis of a hybrid solar-wind energy system and rainwater harvesting for green building planning of a four-story lecture hall building in Padang Pariaman, West Sumatra

Andre Kurniawan[1], Asmitha Bhateja[2]
[1] Departmen of Civil Engineering Dept, Universitas Negeri Padang, Padang, Indonesia
[2] Centre of Research Impact and Outcome, Chitkara, University, Rajpura 140417 Punjab, India
Correspondence: andrekurniawan.sst@gmail.com

Article Info
Article history:
Received March 05th, 2026
Revised June 01th, 2026
Accepted June 07th, 2026

DOI:
https://doi.org/10.68052/SCEJ.v1i2.25

Keyword:
Green Building; Renewable Energy; Solar Photovoltaic; Wind Turbine; Rainwater Harvesting; Energy Efficiency

ABSTRACT
This study presents a technical assessment of green building planning for a four-story lecture hall building with a floor area of 3,880 m², integrating a 177.6 kWp rooftop solar photovoltaic (PV) system, vertical-axis wind turbines (8 × 10 kW), a battery energy storage system, and a sensor-based automatic rainwater harvesting system. Energy and water demand calculations adopted standard green building planning methods, while renewable energy potential was estimated using actual climate data from the Indonesian Agency for Meteorology, Climatology, and Geophysics (BMKG) for 2021–2025, covering rainfall and wind speed in the Padang Pariaman region, West Sumatra. The results show that energy efficiency measures combined with solar PV reduced grid electricity consumption by 58.7% and carbon emissions by approximately 387 tons CO_2 per year. Analysis of actual wind speed data revealed that the site's wind speed is far below the cut-in speed of commercial wind turbines, resulting in a near-zero capacity factor and rendering wind turbine installation technically unfeasible at this location. The rainwater harvesting system, supported by high local rainfall, can meet more than half of the building's clean water demand. This study underscores the importance of validating renewable energy assumptions with actual climate data before making investment decisions in green building planning.

INTRODUCTION

The building sector is one of the largest contributors to energy consumption and carbon emissions in urban environments, particularly educational buildings that operate at high intensity throughout the academic year. The green building concept offers an integrated approach to reducing resource consumption through energy efficiency, renewable energy utilization, and water conservation, without compromising occupant comfort [1].

Green building research in Indonesia has developed rapidly, ranging from Greenship rating assessments of educational buildings [2], evaluation of office building energy consumption intensity to national stakeholder perception surveys on green building rating systems [3], [4]. However, most of these studies assess the performance of buildings that are already operating, or use generic assumptions to estimate renewable energy production, including wind turbine capacity factor assumptions taken from general references without verifying actual local wind conditions. This approach risks producing misleading estimates, given that national wind potential mapping shows that most regions of Indonesia have average wind speeds of only 2–3 m/s [5] , and low-speed wind turbine testing in the city of Padang, West Sumatra, has also confirmed the challenges of wind utilization in this region. This study offers novelty in the form of validating renewable energy assumptions using actual climate data from the Indonesian Agency for Meteorology, Climatology, and Geophysics (BMKG) over the past five years (2021–2025), for both rainfall and wind speed potential, at the planning stage before the building is constructed, so that the calculation results reflect real site conditions rather than mere theoretical assumptions [6].

This study aims to: (1) evaluate the technical feasibility of rooftop solar PV and wind turbine systems as renewable energy sources for a four-story lecture hall building; (2) calculate the three-phase electrical power demand and battery storage capacity of the building; and (3) design a sensor-based automatic water tank system that prioritizes rainwater harvesting. The main contribution of this study is the use of actual BMKG data to replace generic assumptions in wind turbine capacity factor calculations, which proved to change the feasibility conclusion of one of the planned renewable energy components.

From a national policy perspective, the Government of Indonesia, through the National General Energy Plan (RUEN), targets a 23% contribution of new and renewable energy in the national energy mix by 2025, with rooftop solar PV targeted to reach an installed capacity of 3.6 GW in the same period. Commercial and educational buildings are among the primary targets for rooftop solar PV adoption, given their relatively stable load patterns and predominantly daytime operation, which aligns well with solar PV production patterns. However, the shift in rooftop solar PV regulation from Ministerial Regulation of Energy and Mineral Resources No. 26 of 2021 to No. 2 of 2024, which abolished the export-import electricity scheme and replaced it with a quota system, demands more careful planning of self-consumption strategies and energy storage—an aspect that is also addressed in this study [7].

RESEARCH METHODS

This research is a quantitative case study on the technical planning of a four-story lecture hall building with a floor area of 3,880 m² in Padang Pariaman, West Sumatra. The data used include: (1) architectural floor plans for floors 1–4 at a scale of 1:100 to obtain building dimensions and room functions; (2) planned specifications for solar panels (444 units × 400 Wp), vertical-axis wind turbines (8 units × 10 kW), and water tank dimensions (14.2 m × 8.76 m × 2.4 m); and (3) official BMKG climate data for 2021–2025, comprising monthly rainfall and rainy days from the Padang Pariaman Climatology Station, and average annual wind speed from five observation stations in West Sumatra Province[7].

Annual building energy consumption is calculated from the energy consumption intensity (200 kWh/m²/year, referring to the benchmark for air-conditioned educational buildings in Indonesia) multiplied by the floor area, reduced by the efficiency percentage from passive design and energy-saving equipment, then reduced further by renewable energy production to obtain the energy demand from the PLN grid. Solar PV energy production is estimated from the installed capacity multiplied by the annual specific yield, derived from peak sun hours and the performance ratio for a humid tropical climate[8] .

Wind turbine feasibility is analyzed by modeling the average annual wind speed following a Rayleigh distribution, combined with the turbine power curve (cut-in, rated, and cut-out speeds) to obtain a realistic capacity factor estimate [9]. Clean water demand is calculated from the number of daily users multiplied by water consumption per person per day and operational days per year, reduced by efficiency from water-saving sanitary fixtures and automatic sensor faucets. Rainwater potential is calculated from the roof area multiplied by actual rainfall and the roof runoff coefficient.

The main equations used in this study are summarized as follows. Annual building energy consumption before efficiency measures is calculated with:

$$E_{Conventional} = Floor\ Area\ X\ Energy\ Consumption\ Intensity$$

where floor area is in m² and ECI is in kWh/m²/year. Solar PV energy production is calculated with:

$$EPV = Capacity\ (kWp)\ X\ Peak\ Sun\ Hour\ X\ Performance\ Ratio\ X\ 365$$

Wind speed distribution is modeled following the Rayleigh probability density function

$$f(v) = \frac{\pi v}{2\overline{v^2}} \times \exp\left[-\frac{\pi}{4}\left(\frac{v}{\bar{v}}\right)^2\right]$$

where $\bar{v}$ is the average annual wind speed measured by BMKG. The wind turbine power curve is modeled as:

$$P(v) = 0; \quad P(v) = P_{\text{rated}} \frac{v^3 - v_{\text{cut-in}}^3}{v_{\text{rated}}^3 - v_{\text{cut-in}}^3}; \quad P(v) = P_{\text{rated}}$$

The realistic capacity factor estimate is obtained by integrating the product of the turbine power curve and the Rayleigh probability density function, normalized to rated power:

$$F = \frac{\int_0^{\infty} P(v) f(v)\ dv}{P_{\text{rated}}}$$

Annual building clean water demand is calculated with:

$$V_{water} = Number\ of\ Users \times Water\ Consumption\ per\ Person\ per\ Day \times Operational\ Days\ per\ Year$$

Annual rainwater potential follows the standard rainwater harvesting formula [10]

$$V_{rain} = Rainfall \times Roof\ Area \times Runoff\ Coefficient$$

Battery storage capacity requirement is calculated from the critical load, target backup duration, depth of discharge, and round-trip efficiency:

$$C_{battery} = \frac{P_{critical} \times t_{backup}}{DoD \times \eta_{RT}}$$

Meanwhile, the simple payback period of the solar PV investment is calculated with:

$$PP = \frac{Initial\ Investment}{Annual\ Electricity\ Bill\ Savings}$$

RESULTS AND DISCUSSION

The floor plans for floors 1–4 show a building measuring 50.0 m × 19.4 m, with a typical floor area of 970 m², so the total floor area of the four stories reaches 3,880 m². The building consists of classrooms, a computer laboratory, a library, a prayer room, a meeting room/hall, a canteen, a reception area, and two elevators, with an estimated daily user count of approximately 750 people based on the number of classrooms in the floor plan. Details of the building's basic data are presented in Table 1, and the floor plans for all four floors are shown in Figure 1.

Table 1. Building Dimension and Function Data

Parameter	Value
Building width	50.0 m
Building depth	19.4 m
Typical floor area	970 m²
Number of floors	4
Total floor area	3,880 m²
Estimated daily users	≈750 people

Details of the room functions on each floor, which form the basis for estimating the number of users and the building's operational pattern, are presented in Table 2.

Table 2. Room Program per Floor

Floor	Main room functions
Floor 1	Reception, 4 classrooms, computer laboratory, library, meeting room, prayer room, ablution area, canteen
Floor 2	6 classrooms, student activity room, faculty room, prayer room, ablution area
Floor 3	6 classrooms, hall, multipurpose room, prayer room, ablution area
Floor 4	6 classrooms, faculty room, computer laboratory, prayer room, ablution area

Figure 1. Floor Plans of Floors 1–4 of the Lecture Hall Building and Concrete Roof Deck

Figure 1 shows the structural plan of the concrete roof deck (dak beton) that forms the rooftop platform supporting the solar PV array, the wind turbine masts, and the elevated water tank discussed in the following sections. The roof deck dimensions correspond to the building footprint presented in Table 1 (50.0 m × 19.4 m), providing the structural basis for the rooftop equipment loads considered in this study.

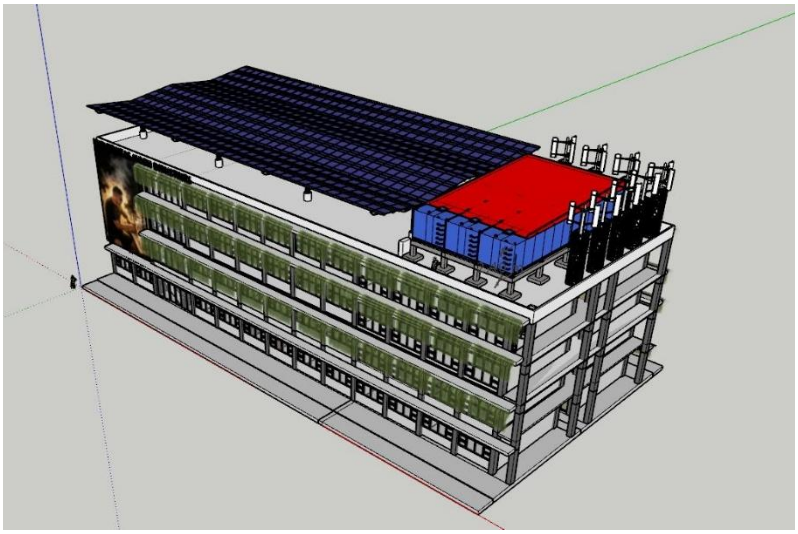

Figure 2. Overall Design Concept Visualization of the Building

Figure 2 shows the initial design concept visualization containing all elements evaluated in this study: rooftop solar panels, vertical-axis wind turbines, a water tank, and a climbing-plant facade on the building's sides as part of a building envelope strategy to reduce direct solar heat exposure and support passive cooling.

It should be noted that the wind turbines shown in this visualization are part of the initial design concept prior to technical feasibility evaluation; based on the actual wind data analysis presented in the following sections, this component is shown to be unfeasible and is no longer part of the recommended final design.

Figure 3. The View of the Vertical Green Facade on the Building Envelope

Figure 3 shows a close-up view of the vegetated (green) facade planned along the building's long façade. This vertical greenery layer functions as an additional passive shading element, reducing solar heat gain on the building envelope while contributing to the building's aesthetic and microclimate, complementing the rooftop renewable energy systems discussed in the following sections.

The rooftop solar PV system is planned to use 444 panel units with a capacity of 400 Wp per unit, giving a total capacity of 177.6 kWp. Assuming a peak sun hour of 4.3 hours per day and a performance ratio of 0.80 for a humid tropical climate, the estimated energy production reaches ≈611 kWh per day, or ≈223,000 kWh per year, equivalent to a specific yield of ≈1,256 kWh/kWp/year (Table 3).

Table 3. Rooftop Solar PV Specification and Estimated Production

Parameter	Value
Number of panels	444 units
Capacity per panel	400 Wp
Total PV capacity	177.6 kWp
Performance ratio	0.80
Specific yield	≈1,256 kWh/kWp/year
Estimated energy production	≈223,000 kWh/year

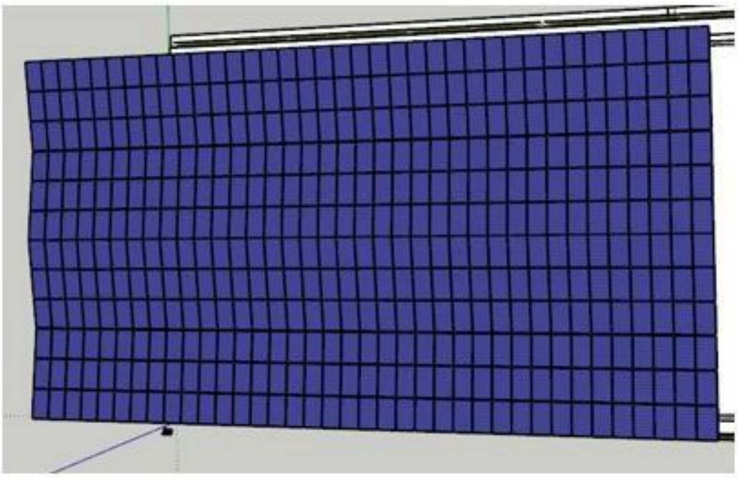

Figure 4. Close-Up View of the Rooftop Solar Panel Array

The initial plan for vertical-axis wind turbines (8 units × 10 kW, 80 kW total) was assumed to achieve a capacity factor of 12–20% based on general references. To verify this assumption, an analysis was conducted on actual wind speed data from five BMKG observation stations in West Sumatra for

2021–2025 (Table 4), focusing on the Sicincin Climatology Station located in Padang Pariaman Regency, where the project is situated.Average

Table 4. Wind Speed Data at BMKG Stations (2021–2025)

Observation station	Average (knots)	Average (m/s)
Sicincin (project site)	1.82	0.94
Minangkabau (airport, reference)	3.09	1.59
Padang Panjang (highland)	4.04	2.08
Teluk Bayur (coastal)	1.16	0.60

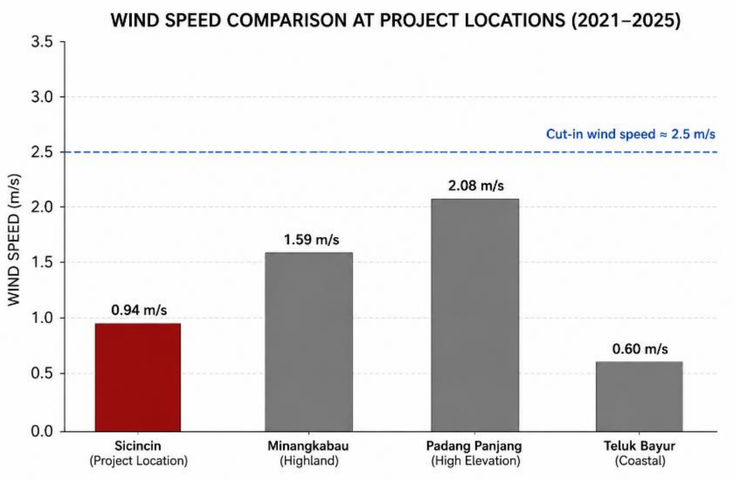

Figure 5. Average Wind Speed Compared to Turbine Cut-In Speed

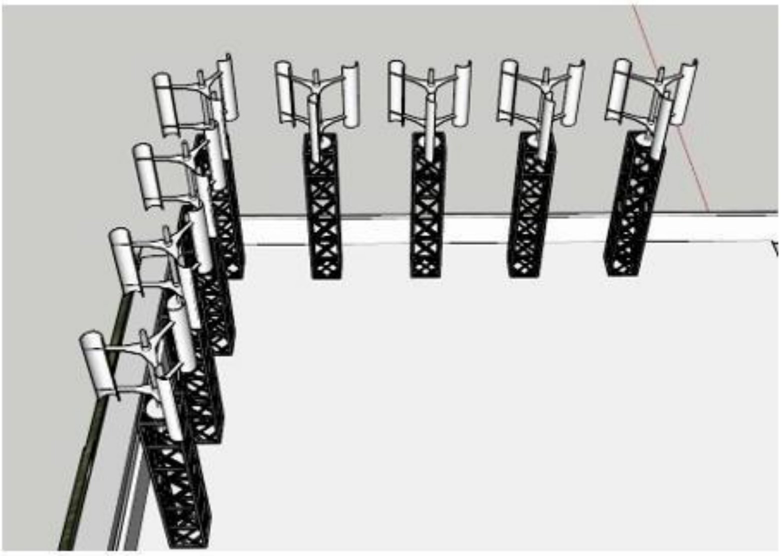

Figure 6. Close-Up View of the Planned Vertical-Axis Wind Turbine Array

Figure 6 illustrates the planned arrangement of the eight vertical-axis wind turbine units on steel lattice masts at the rooftop edge. As discussed below, this configuration is retained in the study purely as a design illustration; the feasibility analysis based on actual wind data indicates that this component should not proceed at the present site.

The average wind speed at Sicincin Station—the station closest to the project site and also the source of rainfall data used in this study is only 0.94 m/s. Even Minangkabau Station, which is located farther away but in the open area of an airport, recorded only 1.59 m/s. Both figures are far below the cut-in speed of small commercial wind turbines, which is generally around 2.5 m/s. By modeling the wind speed distribution using the Rayleigh distribution and combining it with the turbine power curve (cut-in 2.5 m/s, rated 10 m/s, cut-out 25 m/s), the realistic capacity factor estimates presented in Table 5 were obtained.

Table 5. Estimated Wind Turbine Capacity Factor Based on the Rayleigh Model

Parameter	Sicincin	Minangkabau
Probability of wind exceeding cut-in	0.37%	14.30%
Estimated realistic capacity factor	≈0.002%	≈0.213%
Estimated energy production (8×10 kW)	≈12 kWh/year	≈1,490 kWh/year

To test whether raising the turbine mast height could improve feasibility, a sensitivity simulation was conducted using a wind shear power law model with an exponent of 0.20 (representing semi-urban terrain characteristics), as presented in Table 6.

Table 6. Sensitivity of Capacity Factor to Turbine Mast Height (Sicincin Station)

Mast height (m)	Wind speed (m/s)	Estimated capacity factor
10 (BMKG standard height)	0.94	≈0.00%
20	1.07	≈0.01%
30	1.17	≈0.02%
40	1.23	≈0.03%
50	1.29	≈0.05%

The simulation results show that even when the turbine mast is raised to 50 meters—far exceeding the height of this four-story building—the capacity factor remains at 0.05% or lower, which is still insignificant both technically and economically. This indicates that the wind speed limitation at this site is systemic, arising from regional climate characteristics rather than measurement height alone, so raising the turbine mast is not an adequate mitigation measure.

The realistic capacity factor obtained is close to zero, far below the initial assumption of 12–20%, proving that wind turbine installation at this site is technically unfeasible. This finding is consistent with the characteristics of low-lying equatorial tropical wind, which is generally low and inconsistent throughout the year, and confirms that generic capacity factor assumptions without local data verification risk producing significant planning errors. Based on this finding, wind turbine capacity is excluded from the renewable energy calculation, so the total renewable energy that can be relied upon for this building comes practically entirely from the rooftop solar PV system, namely ≈223,000 kWh per year.

The building's three-phase electrical power demand is estimated using a power density approach of 125 VA/m², common for air-conditioned educational buildings in Indonesia [11], plus additional loads for elevators, water pumps, and the canteen kitchen, with a demand factor of 0.65. The estimation results show a power demand of ≈355 kVA, or ≈302 kW at a power factor of 0.85, equivalent to a current of ≈540 A per phase at 380 V, so a PLN connection capacity of 395 kVA is recommended (Table 7).

Table 7. Estimated Three-Phase Electrical Power Demand of the Building

Component	Estimate
Connected load from floor area	485 kVA
Additional load (elevators, pumps, kitchen)	57 kW
Demand factor	0.65
Estimated power demand	≈355 kVA
Recommended PLN connection capacity	395 kVA

The battery storage system is designed to absorb surplus solar PV energy during the day and support critical loads (≈35% of active power, approximately 106 kW) for four hours when PV production is low or during PLN outages. With a depth of discharge of 80% and a round-trip efficiency of 92%, the required battery capacity is estimated at ≈575 kWh using LiFePO4 cells, which are recommended for their long cycle life and better safety for indoor building installation, consistent with a study on battery energy storage for solar PV systems in Indonesia [12], [13], [14] (Table 8). The proposed hybrid architecture channels PV energy to a charge controller that charges the battery first, with an automatic transfer switch (ATS) switching supply to PLN automatically when renewable energy and the battery are insufficient, as illustrated in Figure 7. Wind turbine contribution is not included in this scheme, given the findings in Table 5.

Table 8. Battery Energy Storage System (BESS) Parameters

Parameter	Value
Critical load	≈106 kW
Target backup duration	4 hours
Depth of discharge	80%
Round-trip efficiency	92%
Required battery capacity	≈575 kWh
Cell type	LiFePO4

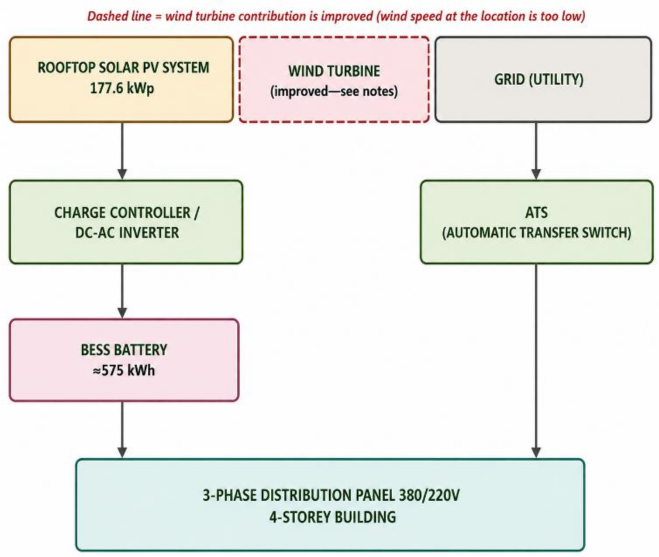

Figure 7. Hybrid System Diagram: Solar PV, Battery, and PLN Grid

Rooftop solar PV regulation in Indonesia has recently undergone a fundamental change. Ministerial Regulation of Energy and Mineral Resources (Permen ESDM) No. 26 of 2021 previously allowed an export-import electricity scheme (net metering) between rooftop PV customers and PLN, in which surplus exported energy could reduce the following month's electricity bill. However, this regulation has been superseded by No. 2 of 2024[15], which abolishes this buy-sell electricity scheme: surplus rooftop PV energy flowing into the grid of a holder of a Business License for Electricity Supply for Public Interest (IUPTLU) is no longer counted as a deduction from the electricity bill (Ministry of Energy and Mineral Resources, 2024). The new regulation also implements a rooftop PV development quota system proposed by the IUPTLU holder and evaluated by the Directorate General of Electricity, which is particularly relevant for large industrial and commercial customers such as this building (connection capacity ≈395 kVA).

The technical implications of this regulatory change are significant for the hybrid system design in this study. Because surplus PV energy exported to the grid no longer has economic value, the optimal strategy is to maximize direct on-site consumption of PV energy (self-consumption) and store surplus production in the battery for later use when PV production is low, rather than relying on export to PLN. This strengthens both the technical and economic justification for the ≈575 kWh battery capacity requirement in Table 8—the battery serves a dual function as both a daytime surplus energy absorber and an emergency power backup, allowing the PV investment's value to be fully optimized through internal building consumption.

Technically, this on-grid hybrid system operates through an inverter that synchronizes the voltage, frequency, and phase of the PV output with the PLN grid before energy is delivered to the building load, equipped with anti-islanding protection that automatically disconnects the PV system from the grid in the event of a PLN disturbance or outage, to protect the safety of personnel repairing the grid. When PLN returns to normal, the system automatically re-synchronizes before reconnecting the PV system to the grid. This configuration ensures that the building can still maximize the use of PV energy for internal needs without relying on export incentives that are no longer in effect, while remaining connected to the PLN grid as the primary backup source beyond the PV and battery capacity.

The battery energy storage system (BESS) is managed through a Battery Management System (BMS) that functions to keep the battery operating within safe and optimal limits. The BMS continuously monitors the voltage of each cell, charge/discharge current, and operating temperature, and performs cell balancing to ensure that all cells in a battery bank are charged evenly, thereby extending the overall battery service life. The BMS also applies overcharge and overdischarge protection by limiting the operational state of charge (SoC) to a range of 10–90% (equivalent to the 80% depth of discharge in Table 8), because repeatedly charging to 100% or fully discharging accelerates the degradation of LiFePO4 cell capacity.

The battery operating strategy follows this priority order: first, PV energy is directed to meet the building's ongoing load (self-consumption); second, surplus PV energy after the load demand is met is used to charge the battery up to a maximum SoC of 90%; third, if the battery is full and PV production still exceeds demand, the surplus energy is exported to the PLN grid within the permitted export capacity without financial compensation, per No. 2 of 2024. At night or when PV production is low (cloudy, rainy conditions), the battery becomes the primary source for critical loads (elevators, computer laboratory, part of the lighting, and water pumps) until the SoC reaches the minimum limit of 10%, after which the ATS automatically switches the critical load supply to the PLN grid. With an estimated capacity of ≈575 kWh and a daily charge-discharge cycle following the PV production pattern, LiFePO4 batteries with a typical cycle life of 4,000–6,000 cycles at 80% DoD are expected to operate for 10–15 years before capacity degrades significantly and partial cell replacement is required.

Overall performance monitoring of the battery and PV system is carried out through a BMS/HMI panel integrated with the building's energy monitoring system (see the limitations section), allowing building management to monitor battery SoC, real-time PV production, load consumption, and grid synchronization status from a single centralized interface.

The water tank system, with a capacity of 298.54 m³ (dimensions 14.2 m × 8.76 m × 2.4 m), is designed to prioritize rainwater as the primary source. Actual rainfall data from the Padang Pariaman Climatology Station for 2021–2025 shows an average of 5,303.9 mm per year with an average of 249 rainy days per year (Table 9), far higher than the generic assumption commonly used (2,300 mm/year), so the rainwater harvesting potential at this site is much greater than initially estimated. With a roof area of 970 m² and a runoff coefficient of 0.85, the annual rainwater potential reaches ≈4,373 m³.

Table 9. Water Tank Capacity and Actual Rainfall Data (2021–2025)

Parameter	Value
Water tank volume	298.54 m³
5-year average rainfall	5,303.9 mm/year
Average rainy days	249 days/year
Roof runoff coefficient	0.85
Annual rainwater potential	≈4,373 m³/year

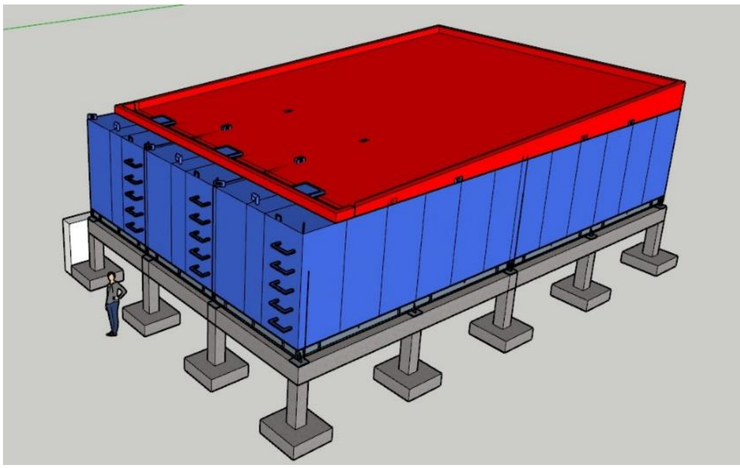

Figure 8. Elevated water tank structure

Figure 8 shows the elevated steel-framed water tank structure supported on a grid of reinforced concrete columns above the rooftop deck, sized to accommodate the 298.54 m³ tank volume specified in Table 9. The elevated configuration keeps the tank clear of the occupied roof area used for the solar PV array and provides gravity-fed pressure for the building's plumbing distribution.

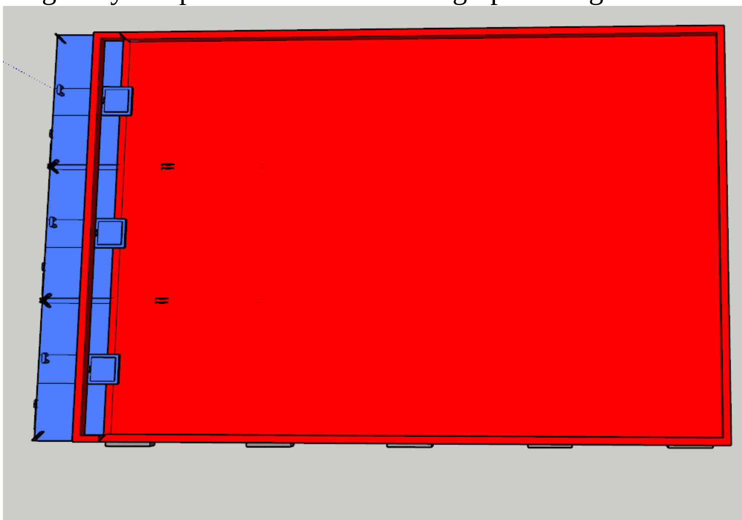

Figure 9. Water Tank Roof Plan (Top View)

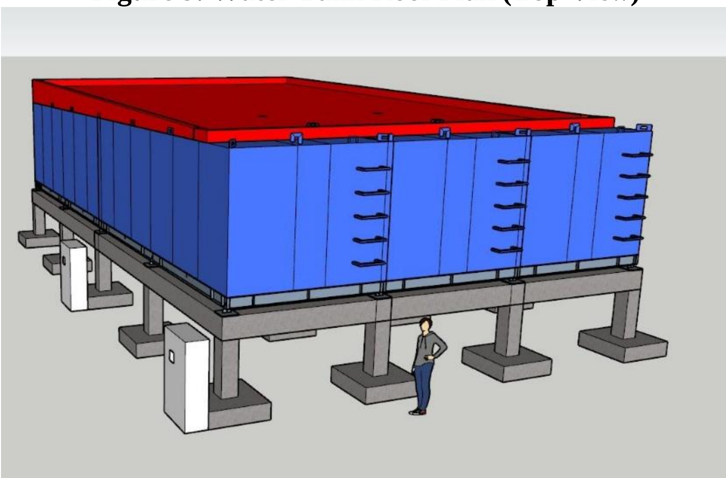

Figure 10. Water Tank Elevation Showing Support Columns and Utility Connections

Figure 9 shows the roof plan of the tank, indicating the access hatches and the modular wall panel layout used for on-site assembly of the tank structure.

Figure 10 shows the tank elevation together with the supporting column grid and the utility connection boxes at ground level, which house the piping and control wiring for the rainwater transfer pump, the groundwater solenoid valve, and the level sensor described in the following control logic.

The tank control system uses an ultrasonic level sensor with a float switch as a mechanical backup to continuously monitor water level, as illustrated in Figure 12. While the water level remains above 30%, the tank continues to receive rainwater supply that has passed through a first-flush diverter and sediment filter, with no additional action taken. When the level reaches the 30% threshold, the controller checks the availability of water in the rooftop rainwater buffer tank; if sufficient, the rainwater transfer pump fills the main tank up to 80% while the groundwater valve remains closed; if insufficient within a certain waiting time, the groundwater well solenoid valve opens as a secondary backup. An additional critical threshold at the 15% level directly activates the groundwater pump as a minimum supply safeguard. Compared to the refill requirement from 30% to 80% (≈149,270 liters), the average annual rainwater supply can meet this requirement within ≈12.5 days, and even in the driest month ever recorded (July 2024, 87.8 mm), the requirement is still met within ≈64 days, demonstrating that rainwater realistically serves as the primary source year-round, with the groundwater well truly functioning only as a secondary backup.

Before entering the main tank, rainwater passes through a staged treatment process to maintain water quality. The first stage is a first-flush diverter, which discards the initial volume of rainwater (typically equivalent to 0.5–2 mm of the first rainfall per roof area) carrying dirt, dust, and contaminants accumulated on the roof surface during dry periods. For a roof area of 970 m², the discarded first-flush volume is estimated at ≈485–1,940 liters per rainfall event, depending on rainfall intensity. The second stage is a sediment filter (50–100 micron mesh) to screen coarse particles such as leaves and sand. The third stage, specifically for water used in applications involving direct user contact such as the ablution area, recommends an activated carbon filter to reduce color and odor, along with an ultraviolet (UV) disinfection module or low-dose chlorination to inactivate pathogenic microorganisms, following the treatment principles of rainwater harvesting systems already implemented in similar buildings in Indonesia[16], [17] .

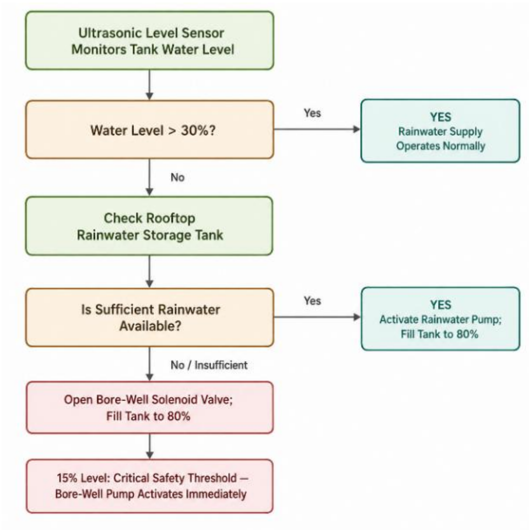

Figure 11. Flow Diagram of the Rainwater Tank Sensor Control Logic

All faucets throughout the building use automatic infrared/motion sensor faucets rather than manual faucets, in line with the reduce principle of the water efficiency strategy. This approach provides greater savings than manual water-saving devices because it eliminates user negligence, so the water efficiency assumption in the following calculation is raised from 25% to 30%. This figure is also consistent with research on automatic lighting systems based on motion and light sensors in multi-story buildings, which reported energy savings of 30–45% without compromising users' visual comfort, supporting the use of automatic sensors as a realistic efficiency strategy across various building systems, both water and energy.

With all the parameters above, the calculation of energy, water, and carbon emissions before and after the application of the green building concept is summarized in Table 10. The application of energy efficiency reduces consumption from 776,000 to 543,200 kWh/year; with the addition of ≈223,000 kWh/year of PV production (wind turbine contribution disregarded based on Table 5), grid energy demand drops to ≈320,200 kWh/year, equivalent to a savings of ≈58.7% compared to conventional conditions and a carbon emission reduction of ≈387.4 tons CO_2 per year, using a national grid emission factor of 0.85 kg CO_2/kWh, which was also used in a study of an off-grid solar PV system in Berau Regency (Arianto & Ismail, 2025). On the water side, sensor faucet efficiency reduces demand from 11,250 to 7,875 m³/year, and rainwater utilization (≈4,373 m³/year) covers ≈55.5% of this demand, leaving ≈3,502 m³/year to be met from the water grid or groundwater well.

Table 10. Summary of Energy, Water, and Carbon Emission Calculations

Component	Before	After
Energy consumption (kWh/year)	776,000	543,200
Energy from the grid (kWh/year)	776,000	≈320,200
Grid energy savings	–	≈58.7%
Clean water demand (m³/year)	11,250	7,875
Water from grid/well (m³/year)	11,250	≈3,502
Carbon emissions (tons CO_2/year)	–	reduced by ≈387.4

This finding is consistent with the green building principle that energy and water efficiency must be prioritized before adding renewable energy generation capacity (Green Building Council Indonesia, 2023), while also showing that renewable energy investment decisions—particularly for wind turbines—must be based on validated actual climate data, not generic assumptions from general references. The difference in grid energy savings results in this study (58.7%) compared to the initial assumption-based estimate (73.2%) is entirely due to the correction of the wind turbine capacity factor, not any change in solar panel performance or building efficiency.

Compared to similar studies, this building's energy consumption intensity after efficiency measures (≈140 kWh/m²/year, from 543,200 kWh/year divided by 3,880 m²) is lower than the energy efficiency index (EEI) of the Sumbawa Regency Office building at 212.143 kWh/m²/year, which has already been categorized as meeting green building criteria [18], indicating that the combination of efficiency measures and solar PV in this plan is competitive compared to an operating government building. The 0.80 PV performance ratio assumption in this study is also consistent with, and conservative compared to, the actual performance ratio of 83% measured for an on-grid solar PV system at SMP N 3 Purwodadi, Central Java, so the PV production estimate in this study is fairly realistic for the planning stage. On the wind aspect, the near-zero capacity factor finding aligns with national wind potential mapping showing that most regions of Indonesia have low wind speeds and low-speed wind turbine testing in the city of Padang, located in the same province as the object of this study, reinforcing the validity of the conclusion that conventional wind turbines are unsuitable for the lowland region of West Sumatra. On the water aspect, the rainwater utilization potential of ≈55.5% of clean water demand in this study aligns with findings from rainwater harvesting at the Sumatra Institute of Technology, which was able to reduce groundwater use by up to 40% of the building's annual demand, confirming that high-rainfall regions on the island of Sumatra consistently have significant potential for rainwater harvesting as a substitute for groundwater[19], [20], [21].

As an initial overview of economic feasibility, assuming a commercial mid-scale solar PV installation cost in Indonesia of approximately IDR 12,000,000 per kWp, the investment for a capacity of 177.6 kWp is estimated at ≈IDR 2.13 billion. With an energy production of ≈223,000 kWh/year and a mid-scale commercial electricity tariff ranging from IDR 1,114.74–1,444.70/kWh, the electricity bill savings are estimated at ≈IDR 249–322 million per year, resulting in a simple payback period of 6.6–8.6 years (Table 11). This figure is comparable to the payback period of an off-grid solar PV study in Berau Regency, which was approximately 8.58 years, although direct comparison should account for differences in system scale, on-grid versus off-grid schemes, and applicable tariff structures.

Table 11. Simple Economic Feasibility Estimate of the Solar PV System

Parameter	Value
Assumed PV installation cost	≈IDR 12,000,000/kWp
Estimated investment (177.6 kWp)	≈IDR 2.13 billion
Annual electricity bill savings	≈IDR 249–322 million
Estimated simple payback period	6.6–8.6 years

This calculation is a rough estimate providing an initial overview of financial feasibility and does not yet account for factors such as financing (loan interest rates), annual solar panel degradation, operation and maintenance costs, net-metering schemes, or potential fiscal incentives for rooftop PV. A more detailed financial feasibility study—covering net present value (NPV), internal rate of return (IRR), and levelized cost of energy (LCOE)—is recommended during the project budget planning stage.

To complement the simple payback period estimate, a 20-year cash flow analysis of the PV system's operational life was also conducted, accounting for an annual solar panel degradation of 0.5%, an annual electricity tariff escalation of 3%, operation and maintenance (O&M) costs of 1% of the investment value per year, and a discount rate of 8% representing the cost of capital for renewable energy projects in Indonesia. Net present value (NPV) is calculated with:

$$NPV = \sum_{t=1}^{n} \frac{CF_t}{(1+r)^t} - Initial\ Investment$$

where CF t is the net cash flow in year t (electricity savings revenue minus O&M costs), r is the discount rate, and n is the project life. The internal rate of return (IRR) is the value of r that makes the NPV equal to zero. The calculation results are presented in Table 12.

Table 12. NPV and IRR Analysis of the Solar PV System (20-Year Operational Life)

Parameter	High-tariff scenario	Low-tariff scenario
Initial tariff	IDR 1,444.70/kWh	IDR 1,114.74/kWh
Net present value (NPV)	≈IDR 1.45 billion	≈IDR 587 million
Internal rate of return (IRR)	≈15.4%	≈11.2%
Payback period (discounted cash flow)	≈7 years	≈9 years
Total 20-year energy production	≈4,254,000 kWh	≈4,254,000 kWh
Total 20-year avoided carbon emissions	≈3,616 tons CO_2	≈3,616 tons CO_2

In both tariff scenarios, the NPV is positive and the IRR (11.2–15.4%) is above the assumed discount rate (8%), indicating that the PV investment in this building is financially feasible in the long term, even though the simple payback period (Table 11) is moderate (6.6–8.6 years). It should be noted that this calculation assumes all PV energy is utilized internally (self-consumption) through a combination of direct use and battery storage, consistent with the absence of export compensation under No. 2 of 2024; if a portion of the PV energy is not absorbed by the building load or battery capacity, the actual economic value will be lower than this estimate.

As an overview of this building's relative position against the green building assessment framework applicable in Indonesia, Table 13 maps this study's design achievements against the six GREENSHIP rating categories from the Green Building Council Indonesia (GBCI), compared with the achievements of similar case studies in the literature discussed earlier).

Table 13. Estimated Design Compliance with GREENSHIP Rating Categories

GREENSHIP category	Design achievement in this study
Appropriate Site Development	Not evaluated in this study (requires site, accessibility, and green open space data)

GREENSHIP category	Design achievement in this study
Energy Efficiency and Conservation	Energy intensity ≈140 kWh/m²/year after efficiency and PV, lower than the 200–250 kWh/m²/year benchmark for similar buildings.
Water Conservation	Rainwater covers ≈55.5% of clean water demand; automatic sensor faucets at all sanitary points
Material Resources and Cycle	Not evaluated (requires construction material specification data)
Indoor Air Health and Comfort	Not evaluated (requires ventilation and natural lighting data)
Building Environmental Management	Planned energy and water monitoring through a centralized BMS/HMI panel

The mapping in Table 13 is indicative and limited to the two categories that are the focus of this study, namely energy efficiency and water conservation; the other four GREENSHIP categories require architectural design and material data that fall outside the scope of this study. Nevertheless, the achievements in these two categories indicate the potential to meet green building criteria on par with, or exceeding, similar case studies in Indonesia, making the pursuit of GREENSHIP New Building certification at a later design stage a relevant step to consider.

This study has several limitations that should be considered when interpreting its results. First, the estimated number of daily users (≈750 people), conventional energy consumption intensity (200 kWh/m²/year), and building efficiency (30%) are planning-stage assumptions derived from general benchmarks and similar literature, not the result of direct measurement on an operating building. Second, the wind turbine feasibility analysis uses average annual wind speed data at the standard BMKG measurement height (generally 10 meters), so seasonal and daily wind speed variation, and wind speed at the actual turbine hub height, are not fully captured, although this has been estimated through a wind shear model. Third, the economic feasibility estimate is simple and does not yet include a sensitivity analysis of fluctuations in PV component prices, battery prices, or electricity tariffs. Further research with primary data measurement after construction is recommended to validate all estimates in this study.

CONCLUSION

This study shows that the application of energy efficiency measures and a rooftop solar PV system in this four-story lecture hall building can reduce grid electricity consumption by ≈58.7% and carbon emissions by approximately 387 tons CO_2 per year, with rainwater potential covering more than half of the building's clean water demand thanks to the high rainfall in Padang Pariaman. However, analysis of actual BMKG wind speed data for 2021–2025 shows that the planned installation of an 80 kW wind turbine capacity at this site is technically unfeasible, because the average wind speed is far below the cut-in speed of commercial turbines, resulting in a realistic capacity factor close to zero. This finding underscores the importance of validating actual climate data before renewable energy investment decisions are made in green building planning, and recommends reallocating wind turbine capacity toward expanded solar PV or battery storage at locations with similarly low wind characteristics.

REFERENCES

[1] J. Lim, F. Fauzan, and E. Oey, “Evaluating green building certification criteria for small health care centre (Puskemas) in Jakarta area – from GREENSHIP to Puske-GREENSHIP framework,” *Smart and Sustainable Built Environment*, vol. 15, no. 3, pp. 1047–1067, Apr. 2026, doi: 10.1108/SASBE-11-2024-0500.

[2] F. Gumilang, “Meta-Analysis of Green Roof Performance Parameters and Policy Readiness in Tropical Indonesia,” *Jurnal Teknologi Lingkungan*, vol. 27, no. 2, pp. 114–126, Jul. 2026, Accessed: Aug. 10, 2026. [Online]. Available: https://ejournal.brin.go.id/JTL/article/view/13263

[3] Y. Li, H. Song, P. Sang, P. H. Chen, and X. Liu, “Review of Critical Success Factors (CSFs) for

green building projects," *Build. Environ.*, vol. 158, pp. 182–191, Jul. 2019, doi: 10.1016/J.BUILDENV.2019.05.020.

[4] Z. Zheng, J. Zhou, Z. Jiaqin, Y. Yang, F. Xu, and H. Liu, "Review of the building energy performance gap from simulation and building lifecycle perspectives: Magnitude, causes and solutions," *Developments in the Built Environment*, vol. 17, Mar. 2024, doi: 10.1016/J.DIBE.2024.100345.

[5] L. M. Parera, A. R. Heluth, M. C. Yesaya, and J. Leuwol, "Wind energy and energy potential assessment on Ambon Island," *Bulletin of Electrical Engineering and Informatics*, vol. 15, no. 1, pp. 884–894, Feb. 2026, doi: 10.11591/EEI.V15I1.10907.

[6] "View of Multiplication Factor of Actual Compressive Strength Relative to the Predicted Compressive Strength Obtained from Hammer Test Results." Accessed: Aug. 10, 2026. [Online]. Available: https://journalcendekia.com/SICEJ/article/view/8/6

[7] "View of Characteristics of Intraslab Earthquake Waves." Accessed: Aug. 10, 2026. [Online]. Available: https://journalcendekia.com/SICEJ/article/view/1/2

[8] "View of Assessment of Awareness and Knowledge of Earthquake Disaster Mitigation among Residential Building Occupants in Padang City." Accessed: Aug. 10, 2026. [Online]. Available: https://journalcendekia.com/asdj/article/view/11/11

[9] "View of Spatial Mapping of Community Earthquake Preparedness in West Sumatra." Accessed: Aug. 10, 2026. [Online]. Available: https://journalcendekia.com/asdj/article/view/15/13

[10] K. Luo and Y. Li, "Assessing rainwater harvesting potential in a humid and semi-humid region based on a hydrological model," *J. Hydrol. Reg. Stud.*, vol. 37, Oct. 2021, doi: 10.1016/j.ejrh.2021.100912.

[11] D. F. Silalahi, A. Blakers, M. Stocks, B. Lu, C. Cheng, and L. Hayes, "Indonesia's vast solar energy potential," *Energies (Basel).*, vol. 14, no. 17, Sep. 2021, doi: 10.3390/EN14175424.

[12] S. R. Sinsel, R. L. Riemke, and V. H. Hoffmann, "Challenges and solution technologies for the integration of variable renewable energy sources—a review," *Renew. Energy*, vol. 145, pp. 2271–2285, Jan. 2020, doi: 10.1016/J.RENENE.2019.06.147.

[13] P. Cosgrove, T. Roulstone, and S. Zachary, "Intermittency and periodicity in net-zero renewable energy systems with storage," *Renew. Energy*, vol. 212, pp. 299–307, Aug. 2023, doi: 10.1016/J.RENENE.2023.04.135.

[14] M. N. Gunawan, Y. Ismail, K. Kunci, P. Air Hujan, and P. Air Berkelanjutan, "STUDY OF RAINWATER HARVESTING IMPLEMENTATION," *Journal of Industrial Engineering, Scientific Journal on Research and Application of Industrial System*, vol. 5, no. 1, pp. 37–47, 2020, Accessed: Aug. 10, 2026. [Online]. Available: http://repository.president.ac.id/xmlui/handle/123456789/3468

[15] "STUDY OF RAINWATER HARVESTING IMPLEMENTATION." Accessed: Aug. 10, 2026. [Online]. Available: http://repository.president.ac.id/handle/123456789/3468

[16] K. Khan, M. T. T. Hermawan, R. Sadono, and W. Wilopo, "The development of micro-zonation of vegetation for conservation of Plawangan Hill in Mount Merapi National Park (MMNP), Indonesia's," *Environmental Monitoring and Assessment 2025 197:8*, vol. 197, no. 8, pp. 878-, Jul. 2025, doi: 10.1007/S10661-025-14181-5.

[17] M. Chang, M. W. McBroom, and R. Scott Beasley, "Roofing as a source of nonpoint water pollution," *J. Environ. Manage.*, vol. 73, no. 4, pp. 307–315, 2004, doi: 10.1016/j.jenvman.2004.06.014.

[18] V. C. Pham *et al.*, "The potential of collected rainwater as an alternative water resource for domestic purpose to mitigate groundwater overexploitation in terms of water quality and people's acceptance," *Environmental Challenges*, vol. 22, p. 101443, Mar. 2026, doi: 10.1016/J.ENVC.2026.101443.

[19] P. Thomson *et al.*, "Rainfall and groundwater use in rural Kenya," *Science of the Total Environment*, vol. 649, pp. 722–730, Feb. 2019, doi: 10.1016/J.SCITOTENV.2018.08.330.